EVS27
Barcelona, Spain, November 17 - 20, 2013

A Novel High-Torque-Density and Wide-Speed-Range Hub Motor for Electric Vehicle Propulsion

M.T. Peng[1], S.H. Chien[1], Y. C. Chung[2], T. S. Liu[2], T.J.Flack[3]
[1]*MSL/ITRI, 195 Chung Hsing Rd., Sec. 4, Chutung, Hsinchu, Taiwan.,mtpeng@itri.org.tw*
[2]*Mechanical Engineering Department, National Chiao Tung University, Taiwan*
[3]*Engineering Department, Cambridge University, UK*

Abstract

This article proposes a novel hub motor, which uses variable electromagnetic (EM) gearing to leverage torque and rotation speed when necessary. Depending on driving conditions, the motor can select a high EM gear ratio or a low EM gear ratio to either increase torque or to increase speed. The technology requires combination of a pole-changeable phase winding and geometry-variable stator profile. The performance of the motor is evaluated and compared with other traditional motors.

Motor, Electric vehicle, Gear

1 Introduction

Electric vehicles have drawn great attention from users by the electrified propulsion system which yields zero carbon emission. One form of propulsion systems allowing more flexible design and space allocation, also exclusive of electric vehicles, is in-wheel drive. In particular to an e-scooter, it is advantageous to use in-wheel drive for obtaining more spare space. However, constraints for an in-wheel motor are quite strict given that only limited weight and space are allowed within a wheel, but the motor is required to produce enough torque and power with high efficiency. Furthermore, the torque and power requirements need to well fit into a wide rotation speed range. More commonly, we can see direct-drive in-wheel motors or geared in-wheel motors. In this article, we propose an in-wheel motor, which is of a direct-drive type but is capable of using electromagnetic gearing. The electromagnetic gearing implemented here is similar to a Vernier motor [1], but with an additional feature of variable EM gear ratios.

2 Motor Design

2.1 Magnetic circuit

The motor mainly differs from a common permanent magnet synchronous Motor (PMSM) in that it has movable pole pieces in the air gap. The moveable pole pieces rotates w.r.t. the motor shaft as a whole and the angle that the pole pieces rest at depends on how the motor's performance is expected. We simply divide the performance into two categories and associate the motor operating with two modes: high-torque mode and high-speed mode. Figures 1 and 2 show the positions of the movable pole pieces relative to the stationary teeth in the high-torque mode and high-speed mode, respectively.

2.2 Stator Winding

In the high-torque or high-speed mode, the stator winding has to be configured accordingly to produce different pole numbers[1], together with different positions of the pole pieces. In the case here, the stator's pole number has to switch between 6 and 12 poles. As shown in table 1, the gear ratio can switch between 2.5 and 5 for the high-speed mode and high-torque mode respectively.

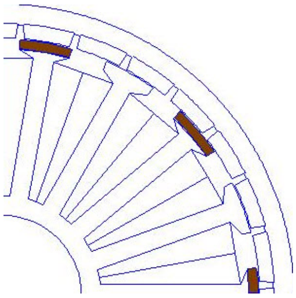

Figure 1: Pole pieces in the high-torque mode

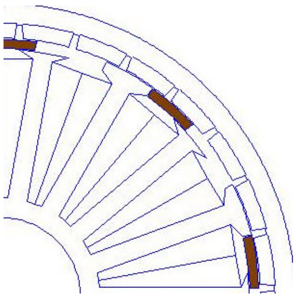

Figure 2: Pole pieces in the high-speed mode

Table 1: Variable gear ratio and motor configuration

	Gear ratio	pole pieces	stator pole number
High-torque mode	5	18	6
High-speed mode	2.5	9	12

It should be noted that in a different design the pole number of the stator winding may be different, following the required gear ratio and the designated number of slots. In another word, the stator pole may switch between two numbers quite arbitrarily and such a winding scheme and circuit may need to be quite specialized. One of such a pole-changeable scheme, quite commonly seen in induction motors, is the Dahlander winding scheme[2], which enable the pole number switch between N and $2N$, for an arbitrary integer N. In the example here, N is equal to 6.

Figure 3 shows coil number and its slot location, where p denoted the positive terminal for the current to flow into. Figures 4 and 5 show three-phase Y-type windings for the 6-pole and 12-pole configurations respectively. By symmetry, we only show how the U-phase winding is reconfigured. It is noted that in transforming from 6-pole to 12-pole configuration, we only need to reverse the current direction in one half of the coils, that is coil 6, 12 and 18. The current direction in 3, 9 and 15 remains the same.

3 Performance evaluation

Table 2 shows the dimension of the motor and other major parameters.

As shown in the winding figures 4 and 5, each phase winding has 3 coils connected in series

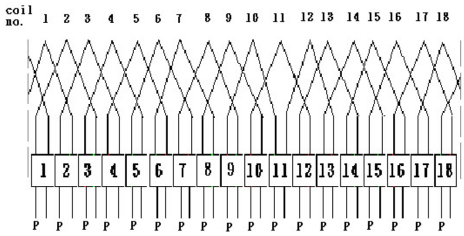

Figure 3: Winding diagram

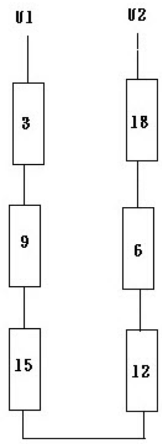

Figure 4: Winding configuration for 6-pole field

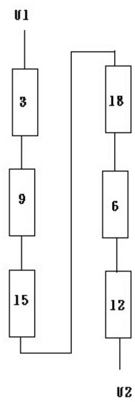

Figure 5: Winding configuration for 12-pole field

Table 2: Parameters

Rotor outer diameter (mm)	240
Rotor inner diameter (mm)	220
Stator outer diameter (mm)	210
Stack length (mm)	60
Number of slots	18
Number of turns	60

and has 2 parallel branches. We can solve the following motor equation for evaluating its performance, and use the magneto-static finite element analysis to calculate winding inductances and rotor-driven flux linkages. The motor equation is expressed in terms of phasor with its magnitude in rms unit:

$$V = Ri + X_S i + E \tag{1}$$

,where R is the phase resistance, X_S is the synchronous reactance and E is the back EMF.
The input voltage is $V = V_M e^{j\theta_V}$, where $V_M = \frac{\sqrt{3}V_{DC}}{2\sqrt{2}}$ and θ_V is the phase lag.
The back EMF E is assumed to be sinusoidal, which is proportional to the peak rotor flux linkage ψ_m, the pole-pairs of permanent magnets p and the mechanical rotor speed ω_m. Furthermore, we assumed the phasor E aligns with the imaginary axis, that is $\theta_E = \frac{\pi}{2}$.

$$E = \psi_m p \omega_m e^{j\theta_E} \tag{2}$$

,where θ_E is the phase lag.
In the analysis, through properly adjusting the phase lag θ_V of the input voltage, we can control the current's phase, and enable the field-oriented control in which the d-axis current or the real projection of the current, becomes zero.
Knowing input electric power to the 3 phase windings and the output shaft speed, we can calculate the motor torque by the equation 3:

$$T = \frac{3EI}{\omega_m} \tag{3}$$

The maximum torque of 250 Nm in the high-torque mode has been verified by experiment. With the above evaluating scheme, torque-speed curves can be calculated, as in figures 9 and 10.

4 Benchmark motors for performance comparison

Two benchmark motors are devised. For having similar voltage and current ratings, we use the same motor stator, which has 12-pole configuration. Figure 8 shows the cross-section of the motor. The first benchmark motor is an permanent magnet synchronous motor with 12-pole magnets on the rotor. The second benchmark motor is a gear motor consisting of the first benchmark motor and a 3:1 mechanical reducer.
Figures 9 and 10 show the speed-torque and speed-power curves under various DC link voltage for the first benchmark motor.

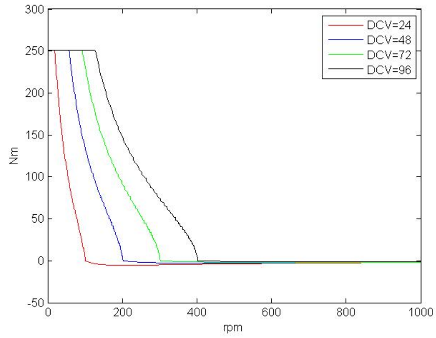

Figure 6: TN curve for the high-torque mode

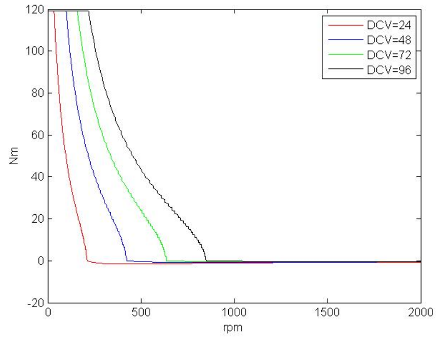

Figure 7: TN curve for the high-speed mode

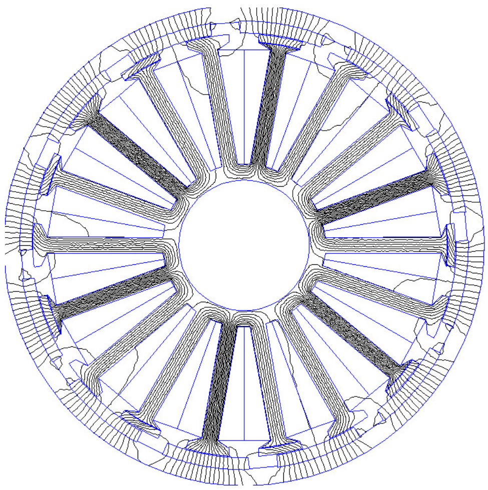

Figure 8: Cross-section and flux lines driven by 12-pole surface-mount permanent magnets

In the vehicle platform, an e-scooter, for the comparison, we first found that the second benchmark motor has difficulty in reaching a higher

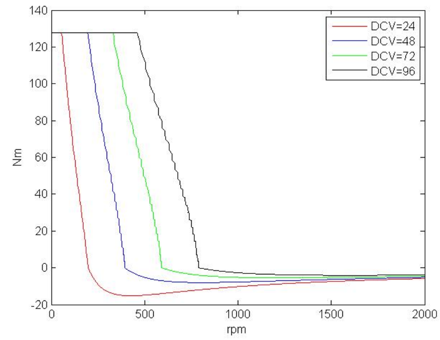

Figure 9: Torque curve of the first benchmark motor

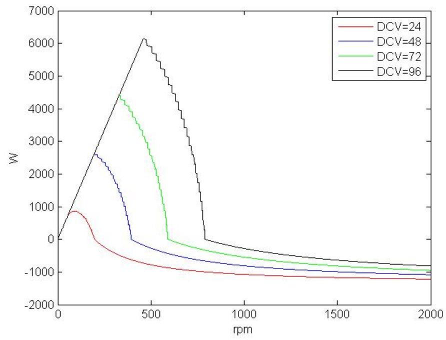

Figure 10: Power curve of the first benchmark motor

speed, such as over 40 kph, since by connecting with a reducer the actual rotor speed has to increase threefold for the same shaft output speed and the rotor speed has exceeded that allowed in the field-oriented control, compared with other direct-drive motors. To enable the comparison for the performance, we have to change 3-series/2-parallel winding as in the first benchmark motor to 1-series/6-parallel configuration. Figures 11 and 12 show the speed-torque and speed-power curves under various DC link voltage for the second benchmark motor. We further assume that the reducer used in the second benchmark motor is of the planetary type with efficiency 80% at a rated torque output about 100 Nm.

5 Result and discussion

The vehicle under the propulsion test is an e-scooter, which has a weight 180 kg and its wheel radius is 0.215 m. The efficiency calculation is done through averaging all efficiency figures at various speeds and driving conditions. The power loss is assumed only including the copper loss. In the efficiency averaging, the driving duty is assumed evenly distributed over 3 driving conditions: 20 kph and 40 kph on a general road and also 20 kph climbing a 20% slope. It should be noted that a higher cruise speed more than 40 kph is possible through using the field-

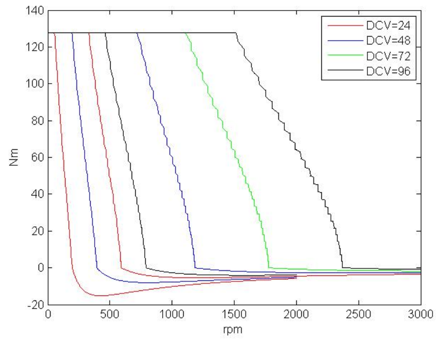

Figure 11: Torque curve of the benchmark motor with parallel connection

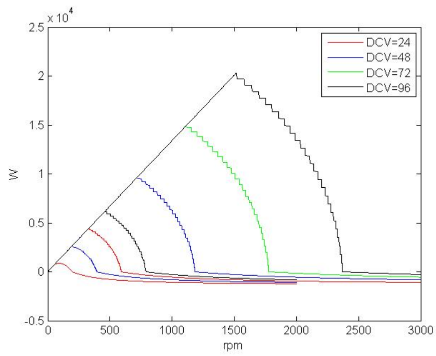

Figure 12: Power curve of the benchmark motor with parallel connection

weakening technique. However, for simplicity in this article we only consider the vehicle speed range without field weakening. 96 V DC-link voltage is used here.
We first compile the voltage and current ratings for each motor, as shown in table 3. The maximum current through each stator coil is 30 A (rms), and the total phase current is 30 A multiplied by the number of parallel branches. We observe that the gear motor would require a motor controller with a larger power module capable of supplying 180 A (rms) line current, compared with only 60 A in other motors. Table 4 lists the required motor torque for each driving condition, from which we are able to determine the required current and the motor efficiency by referring to their speed-torque curves.

Table 3: Voltage and current ratings

Motor type	DC-link voltage (V)	Phase current (A rms)
Benchmark I	96	60
Benchmark II	96	180
EM gearing motor	96	60

Table 4: Required torque for the vehicle

Speed (kph)	20	40	20 (20%slope)
Torque (Nm)	7	13	130

The efficiency is compared in table 5. It is noted that the gear motor has the lowest efficiency compared with other motors due to the assumed low 80% efficiency of the reducer. We also investigate using higher-efficient reducers. In these cases the gear motor has efficiencies of 88% and 93% corresponding to using the 90%- and 95%-efficient reducers respectively.

Table 5: Efficiency comparison

Motor type	Average efficiency
Benchmark I	86%
Benchmark II	78.3%
EM gearing motor	94%

6 Conclusion

In this article, we propose a EM gearing motor, which can change the gear ratio according to the driving conditions. The performance of the motor is evaluated. Its effects as an in-wheel motor on vehicle propulsion, in particular voltage/current ratings and energy conversion efficiency, have been compared with some benchmark motors. The result shows that the idea of variable EM gear ratios is quite promising and the motor have advantages in the application of vehicle propulsion.

Acknowledgments

We are grateful to the support of MOEA, Taiwan for this research project in ITRI.

References

[1] A. Toba and T. A. Lipo, *Generic Torque-Maximizing Design Methodology of Surface Permanent-Magnet Vernier Machine*, IEEE TRANSACTIONS ON INDUSTRY APPLICATIONS, VOL. 36, NO. 6, 2000, 1539-1546.

[2] M. van der Giet et al., *Induction motor with pole-changing winding for variable supply frequency*, IEEE , 2007, 1484-1489.

Authors

Dr. M.T. Peng received his B.S. degree in 1990 from Chung Yuan University, Taiwan and Ph.D. degree in 2004 from Cambridge University, UK. He is currently working in MSL/ITRI, Taiwan. His research interest is in electric motor and dynamical system identification.

Dr Chien's research interests are in the area of variable structure control, adaptive control and fuzzy control theory. Dr. Chien is now working in Mechanical and System Research Lab. Industrial Technology Research Institute, Taiwan.

Y. C. Chung received the B.S. degree in Mechanical Engineering from National Taipei University of Technology, Taipei, Taiwan, in 2011, and currently working toward the M.S. degree in Mechanical Engineering of National Chiao Tung University, Taiwan. His research interests include the design, modeling, and control of electric machines.

Professor T. S. Liu obtained his B.S. degree in 1979 from National Taiwan University, Taipei, M.S. degree in 1982 from University of Iowa, U.S.A., and Ph.D. degree in 1986 from University of Iowa, U.S.A., all in Mechanical Engineering. Professor Liu has been teaching in National Chiao Tung University, Taiwan since 1987. His research interest lies in electric motor, mechatronics, and automatic control.

Dr Flack obtained his BSc in Electrical Engineering from Imperial College, London, in 1986 and three years later his PhD from the same institution. Since then he has worked at the Cambridge University Engineering Department and his current research interests include the modelling of automotive electrical systems, the design and optimisation of electromagnetically-geared motors, the development of the BDFM as a potential candidate for wind power, and applied superconductivity.